
Article:
Dufresne, Emilie orcid.org/0000-0001-9290-7037, Harrington, Heather A, Kevrekidis, Panayotis G et al. (2 more authors) (2020) On Some Configurations of Oppositely Charged Trapped Vortices in the Plane. Advances in Applied Mathematics. ISSN 0196-8858

https://doi.org/10.1016/j.aam.2020.102099

ON SOME CONFIGURATIONS OF OPPOSITELY CHARGED TRAPPED VORTICES IN THE PLANE

EMILIE DUFRESNE, HEATHER A HARRINGTON, JONATHAN D. HAUENSTEIN, PANAYOTIS G KEVREKIDIS, AND PAOLO TRIPOLI

Abstract. Our aim in the present work is to identify all the possible standing wave configurations involving few vortices of different charges in an atomic Bose-Einstein condensate (BEC). In this effort, we deploy the use of a computational algebra approach in order to identify stationary multi-vortex states with up to 6 vortices. The use of invariants and symmetries enables deducing a set of equations in elementary symmetric polynomials, which can then be fully solved via computational algebra packages. We retrieve a number of previously identified configurations, including collinear ones and polygonal (e.g. quadrupolar and hexagonal) ones. However, importantly, we also retrieve a configuration with 4 positive charges and 2 negative ones, which is unprecedented, to the best of our knowledge, in BEC studies. We corroborate these predictions via numerical computations in the fully two-dimensional PDE system of the Gross-Pitaevskii type which characterizes the BEC at the mean-field level.

1. Introduction

The explosion of interest in the theme of atomic Bose-Einstein condensates (BECs) [56, 54, 37] has had significant implications in the study of associated nonlinear coherent structures, including vortices, as well as vortex lines and vortex rings [55]. In particular, settings involving the emergence and precessional dynamics of one or few vortices (see e.g. [4, 29, 13, 52, 24, 46, 51] for some typical examples), as well as the exploration of higher charged vortices and their potential decay to lower charged ones (see, e.g., [60, 34]) have been topics that garnered considerable interest within the atomic and nonlinear communities and motivated numerous associated experiments. Vortical patterns not only in two but also in higher dimensions (e.g., filaments in the form of lines and rings in 3d) were also produced by means of dynamical instabilities such as the extensively studied transverse instability [3, 20, 38]. The topic of one [36] and few vortices (possibly of different signs [58, 26, 50, 28]) remains under active experimental investigation still to this day.

The study of BECs at the mean-field level at (and very close to) zero temperatures is well established to be described by the famous Gross-Pitaesvkii (GP) partial differential equation (PDE) [56, 54, 37]. When rewriting the equation for the complex wavefunction into a system of equations for the density ρ and velocity $v = \nabla\phi$ (where ϕ is the phase of the complex field) one obtains a system strongly reminiscent of the

Date: August 3, 2020.

2010 *Mathematics Subject Classification.* 81U30.

Key words and phrases. Bose-Einstein condensates, standing wave vortex configurations in the plane, symbolic computational methods, invariant theory.

Euler equations in fluid dynamics. For a recent, detailed account of this connection, see, e.g., [12]. The role of the quantum features arises through the so-called quantum pressure term. This analogy can be utilized to approximate the vortex dynamics and interactions within the GP system by those of point vortices in the fluid setting; for a recent discussion of how to utilize configurations of the latter to prove the existence of steady or co-traveling states in the former, see, e.g., [41]. There is a history of connections between the theory of different types of polynomials and the study of vortices in fluids [35, 6, 5]. Recent years have seen an attempt to extend such considerations to the more complex (in that it bears an external trapping potential) setting of BECs, including extensions of relevant multi-vortex configurations [7] and associated polynomial generating function techniques [8]. It is along these lines of associating the equations for the vortex positions (and their conjugates) with a system of polynomial equations and using symbolic algebraic techniques to tackle the latter that we proceed in the present study.

Solving polynomial equations is central to algebraic geometry. Over the past century many approaches have been developed, and with them, many algorithms. Fifty years ago, Buchberger proposed the Gröbner basis algorithm for solving polynomial systems [14], which was improved by Faugère [21], and is now the central tool in computational algebraic geometry (see, for example, [15]). Gröbner bases are implemented in several packages, from general symbolic software such as Mathematica [33] and Maple [1], to specialised software such as Magma [11], Singular [17] and Macaulay2 [27]. Despite the computational complexity of Gröbner bases being double exponential in the worst case, there has been much success in using Gröbner basis techniques to solve problems in a wide range of applications including shear flow, nonlinear mechanics, chemical reactions, dynamical systems, statistics, systems biology and computer vision, among many others [53, 42, 19, 25, 57, 39, 30, 2].

Our aim here is to use such methods to *fully* characterize all possible solutions of the system of vortex equations for stationary configurations involving up to 5 vortices and offer all the computationally tractable solutions for 6 vortices. There are two natural avenues for obtaining polynomial equations to describe the vortex positions. We either consider the conjugate variables of the vortex positions or separate the equations in terms of real and imaginary parts. However, solving these systems using standard Gröbner basis approaches is computationally out of reach [43] (see Table 2). The next step is then to attempt to exploit any symmetries in the equations. The system of equations for the vortex positions (see Equation 6) is symmetric in the variables, that is, it is invariant under the action of a permutation group. However individual equations in the system are not invariant. If the system was given by algebraic equations, then theoretically there is a system consisting of invariant equations which has the same solutions and can be rewritten in terms of a basic set of invariants (see [62, 18]). However using the standard algorithms in invariant theory is, again, computationally intractable for the vortex equations.

While all the general approaches fail for the vortex problem, one can tailor ideas from computational algebra and invariant theory to gain new insight about vortex configurations. For example, Faugère and Svartz [22] proposed a general approach

for systems with an action of the permutation group and they specialised their approach to find configurations of up to 8 single charged vortices. Here we extend this analysis to the equally relevant case of vortices with opposite charges. While vortex configurations of the same charge are rigidly rotating, those with opposite charges can be genuinely stationary [37]. For the latter, we specifically first construct a family of symmetric equations in the variables and their conjugates whose set of common zeros includes the solutions to the ODE approximation of the vortex problem. Next, from these equations we deduce a set of equations in the elementary symmetric polynomials in the variables. The common zero set of these equations, again, includes the solutions to the ODE approximation of the vortex problem. Finally we solve the system in the elementary symmetric polynomials and we convert the solutions into the original variables. Practical considerations presently prohibit an exhaustive study of larger (than 6, as considered herein) numbers of vortices, although this is an interesting and practically important topic for further study. Once we have these solutions, our final step is to come full circle and check the existence of such configurations in the original PDE problem. This is explored in some detail (and at different levels of approximation) in Section 5.

Our paper is organised as follows. In Section 2 we explain how to translate the underlying PDE to polynomial systems. The theoretical results and proofs of the two charged vortex problem using algebraic approaches is presented in Section 3. In Section 4 we give the results from the computational algebra for the configurations of vortices and the benchmarking of the various approaches, showing that the direct approaches fail. In Section 5, we show that numerical solutions of the PDE corroborate the presently identified solution, as well as all the ones for smaller vortex numbers. Finally, in the last section, we give conclusions and suggest some directions for future work.

2. From vortices to algebra

The original PDE problem involves identifying standing wave solutions of the two-dimensional Gross–Pitaevskii equation of the form [56, 54]:

$$iu_t = -\frac{1}{2}\Delta u + |u|^2 u + Vu, \tag{1}$$

where Δ represents the two-dimensional Laplacian and the external trapping potential $V(r)$ is assumed to be parabolic, i.e., $V(r) = \frac{1}{2}\Omega^2(r)$, where $r = x^2 + y^2$ and Ω is the trap. Notice that this dimensionless version of the GP equation has been obtained through well-established reductions of the dimensional one, as detailed, e.g., in [37]. We use solutions of the form $u(x, y, t) = e^{-i\mu t}U(x, y)$ with chemical potential μ and subsequently solve the nonlinear steady state problem for $U(x, y)$ via a fixed point iteration.

When identifying solutions bearing vortices, we can attempt to capture the effective dynamics of the vortices through the following ordinary differential equations:

$$i\dot{z}_j = S_j\omega_{pr}z_j + \sum_{1\le k\ne j\le n} \frac{S_k}{\bar{z}_j - \bar{z}_k.} \tag{2}$$

Here S_j are the charges of the vortices, ω_{pr} is their precession frequency inside the parabolic trap, i is $\sqrt{-1}$ and the complex number z_j represents the planar position of the j-the vortex. Near the center of the trap it is reasonable to assume that vortices have a nearly constant precession frequency ω_{pr}. This has been described, e.g., recently in [36]. The second term captures the inter-vortex interactions of the j-th vortex with all the other vortices (summed over k). Notice that this is a velocity-induced interaction, i.e., each vortex induces a velocity field at the location of all the others, as is the case for vortices in inviscid, incompressible fluid (point) vortices. Notice that this description is progressively more accurate for larger values of the chemical potential μ, whereby the vortices approach the limit of point vortices with (decreasing width and thus) no internal structure.

However, the ground state of the system, i.e., the background over which the vortices are located decreases in its density as one moves radially outwards, due to the presence of the parabolically confining external potential. As has been extensively examined since early on [23] (see also the recent discussion of [36]), this has an implication of radially increasing the precession frequency according to

$$\omega_{pr}(|z_j|) = \frac{\omega_{pr}(0)}{1 - \frac{V(|z_j|)}{\mu}}. \tag{3}$$

In turn, this leads to the amended version of the equations of motion as:

$$i\dot{z}_j = S_j \frac{\omega_{pr}(0)}{1 - \frac{V(|z_j|)}{\mu}} z_j + \sum_{1 \leq k \neq j \leq n} \frac{S_k}{\bar{z}_j - \bar{z_k}}. \tag{4}$$

However, it turns out that the interactions between the vortices are also affected by the presence of the external potential. In particular, the interactions between the vortices as characterized in Equation (2) assume the presence of *a homogeneous background* in which the vortices move. A spatially inhomogeneous background, present in the case of the trap, modifies (i.e., *screens*) the inter-vortex interactions in a way that has been recently captured, e.g., in [64]. As discussed in this work and its references, the effect of the presence of a spatially inhomogeneous background can, in turn, be captured by a modulating factor, leading to a further revised form of the equations. The latter account for the inhomogeneous background in both the individual vortex precession and in the inter-vortex interactions by equations:

$$i\dot{z}_j = S_j \frac{\omega_{pr}(0)}{1 - \frac{V(|z_j|)}{\mu}} z_j + \sum_{1 \leq k \neq j \leq n} \frac{V(|z_j|)}{V(|z_k|)} \frac{S_k}{\bar{z}_j - \bar{z_k}}. \tag{5}$$

Our aim in the present work is to explore equilibrium multi-vortex configurations involving vortices of both charges, i.e., with $S_j = \pm 1$. In particular, we will more specifically assume that we have M vortices with $S_j = 1$ and N vortices with $S_j = -1$. We will denote the former with the positions $x_1, \ldots, x_M$ in the complex plane $\mathbb{C}$ and the latter with the positions $y_1, \ldots, y_N$ in the same plane. Our analysis will take place at the level of the simplest equation for the vortices, namely Equation (2). However, in Section 5, we will illustrate the connections of this setting with the full original problem, as well as the more elaborate (and more accurate) variations of the form of Equations (4) and (5). At the level of Equation (2), splitting the equations

for positive and negative charges, according to the symbolism above, we obtain the steady state formulation:

$$\begin{cases} \overline{x_i} = -\displaystyle\sum_{\substack{j\neq i\\ j=1}}^{M} \frac{1}{x_i - x_j} + \sum_{j=1}^{N} \frac{1}{x_i - y_j}, \quad i = 1, \dots M, \\ \overline{y_i} = -\displaystyle\sum_{\substack{j\neq i\\ j=1}}^{N} \frac{1}{y_i - y_j} + \sum_{j=1}^{M} \frac{1}{y_i - x_j}, \quad i = 1, \dots N. \end{cases} \tag{6}$$

Note that the solutions of this system present many symmetries:

Lemma 2.1 (Symmetries of the vortex equations)**.** *The set of solutions to the system* (6) *is invariant under up to the following three different group actions.*

- *The product of symmetric groups $S_M \times S_N$ acts by permuting the variables via $(\sigma_1, \sigma_2) \cdot x_i = x_{\sigma_1(i)}$, $(\sigma_1, \sigma_2) \cdot y_j = y_{\sigma_2(j)}$.*
- *The group of complex numbers of modulus 1 acts via $\lambda \cdot x_i = \lambda x_i$ and $\lambda \cdot y_i = \lambda y_i$. This corresponds to rotations of the complex plane around the origin.*
- *The cyclic group of order 2 acts via conjugation. This correspond to reflection of the complex plane with respect to the real axis.*

Moreover, when $M = N$, the set of solutions to the system (6) *is invariant under an additional group action.*

- *The cyclic group of order 2 acts by exchanging x_i and y_i.*

Proof. This is verified via straightforward computations. □

2.1. **Obtaining algebraic equations: direct approaches.** System (6) fails to be algebraic because of the presence of the conjugation operator. In the next two subsections, we discuss two direct approaches for converting this problem into an algebraic problem, which provides the possibility to use algebraic methods. Both approaches end up doubling the number of variables and equations. We show in Section 4 that these approaches cannot succeed in their practical implementation, unless the resulting system is not suitably reduced.

2.1.1. *Conjugate variables.* A first method of converting system (6) to an algebraic system is to introduce a new sets of variables $X_1, \dots X_M, Y_1, \dots Y_N$ representing the complex conjugates of the variables $x_1, \dots x_M, y_1, \dots y_N$. Therefore we obtain the following equations:

$$(E_i^{(x)}) \qquad X_i = -\sum_{\substack{j\neq i\\ j=1}}^{M} \frac{1}{x_i - x_j} + \sum_{j=1}^{N} \frac{1}{x_i - y_j}, \quad i = 1, \dots M,$$

$$(E_i^{(y)}) \qquad Y_i = -\sum_{\substack{j\neq i\\ j=1}}^{N} \frac{1}{y_i - y_j} + \sum_{j=1}^{M} \frac{1}{y_i - x_j}, \quad i = 1, \dots N,$$

$$(\bar{E}_i^{(x)}) \qquad x_i = -\sum_{\substack{j\neq i\\ j=1}}^{M} \frac{1}{X_i - X_j} + \sum_{j=1}^{N} \frac{1}{X_i - Y_j}, \quad i = 1, \dots M,$$

$$(\bar{E}_i^{(y)}) \qquad y_i = -\sum_{\substack{j\neq i\\ j=1}}^{N} \frac{1}{Y_i - Y_j} + \sum_{j=1}^{M} \frac{1}{Y_i - X_j}, \quad i = 1, \dots N.$$

We now have $2(M+N)$ equations in $2(M+N)$ variables.

Remark 2.2. Each of the symmetries described in Lemma 2.1 extends to the solutions of this new system naturally.

Polynomial equations for this system are obtained from these equations by clearing the denominators. Let us denote by D the discriminant $D = \prod_{i\neq j}(x_i - x_j) \cdot \prod_{i,j}(x_i - y_j) \cdot \prod_{i\neq j}(y_i - y_j)$ and by $\bar{D}$ the discriminant in the conjugate variables $\bar{D} = \prod_{i\neq j}(X_i - X_j) \cdot \prod_{i,j}(X_i - Y_j) \cdot \prod_{i\neq j}(Y_i - Y_j)$. Since we cleared the denominators, we need to exclude solutions where D and $\bar{D}$ are zero. This is done by introducing two new variables h and H and by adding to the system the equations $h \cdot D - 1 = 0$ and $H \cdot \bar{D} - 1 = 0$. If we solve the system without doing this step, then we will find infinitely many solutions. Finally, to reduce the dimension of the set of solutions, we need to remove the symmetry given by the multiplicative action of complex numbers of modulus 1 mentioned in Remark 2.2. To do so, we impose the condition that some non-zero variable of the system is real. We do this in the following way:

(1) we subdivide the system into two subsystems corresponding to the cases $x_1 = 0$ and $x_1 \neq 0$. In particular, the first subsystem is obtained by adding the new equation $x_1 = 0$, the second subsystem is obtained by adding a new variable a and the new equation $a \cdot x_1 - 1 = 0$,
(2) we add the new equation $y_1 - Y_1 = 0$ to the subsystem where $x_1 = 0$ (i.e., we assume $y_1 \neq x_1 = 0$ is real) and we add the new equation $x_1 - X_1 = 0$ to the subsystem where $x_1 \neq 0$ (i.e., we assume $x_1 \neq 0$ is real).

The two systems so obtained can be solved using standard algebraic geometric tools and in the cases considered yield finitely many solutions. To get the solutions of system (6) we now just need to select those solutions where $x_i = \bar{X}_i$ and $y_i = \bar{Y}_i$.

2.1.2. *Real and imaginary parts.* An alternative approach to describe system (6) as a polynomial system consists in doubling up the number of equations and variables by considering real and imaginary parts separately. We introduce $2M + 2N$ variables

$a_1, \dots, a_M, b_1, \dots, b_M, c_1, \dots, c_N, d_1, \dots d_N$. We substitute the variables in system (6) via $x_i = a_i + \sqrt{-1}b_i$ and $y_i = c_i + \sqrt{-1}d_i$ and we clear the denominators. Separating the real and imaginary parts of the resulting $M + N$ equations, we get a system of $2M + 2N$ real polynomial equations, two for each equation of system (6). Finding solutions to system (6) is now equivalent to finding real solutions to this new system. The discriminant D can be written as $D = \prod_{i\neq j}(a_i + \sqrt{-1}b_i - a_j - \sqrt{-1}b_j) \cdot \prod_{i,j}(a_i + \sqrt{-1}b_i - c_j - \sqrt{-1}d_j) \cdot \prod_{i\neq j}(c_i + \sqrt{-1}d_i - c_j - \sqrt{-1}d_j)$. The discriminant D can be written as a sum $D = D_{\text{re}} + \sqrt{-1}D_{\text{im}}$, where D_{re} and D_{im} are real polynomials. We now add to the systems an extra variable h and the equation $h \cdot D_{\text{re}} \cdot D_{\text{im}} - 1 = 0$ to ensure that the real and the imaginary part of D are not both zero. Here, the multiplicative action of complex numbers of modulus 1 becomes the group of rotations around the origin in the real plane. We get rid of this 1-dimensional symmetry by requiring that one of $x_1 = a_1 + \sqrt{-1}b_1$ or $y_1 = c_1 + \sqrt{-1}d_1$ is purely imaginary:

(1) we subdivide the system into two subsystems corresponding to the cases $a_1 + \sqrt{-1}b_1 = 0$ and $a_1 + \sqrt{-1}b_1 \neq 0$. In particular, the first subsystem is obtained by adding the new equations $a_1 = 0$ and $b_1 = 0$, the second subsystem is obtained by adding a new variable k and the new equation $k \cdot a_1 \cdot b_1 - 1 = 0$,
(2) we add the new equation $c_1 = 0$ to the subsystem where $a_1 + \sqrt{-1}b_1 = 0$ and we add the new equation $a_1 = 0$ to the subsystem where $a_1 + \sqrt{-1}b_1 \neq 0$.

Real solutions of this system can now be obtained either by finding all complex solutions with symbolic methods and then picking out the real solutions, or by approximation with numerical algebraic geometry (see Section 4).

3. Obtaining algebraic equations: exploiting the symmetries

In this section we exploit the invariance of system (7) under the action of $S_M \times S_N$ to obtain a new set of equations. The equations we obtain are not simpler to the eye, far from it, but will prove to be better for symbolic computations (See Section 4).

In the rest of this section we explain how to exploit the symmetries described in Lemma 2.1 and Remark 2.2 in order to go further with computations than what can be achieved with the direct approaches. We focus on the action of the product of symmetric groups. Our starting point is the conjugate variables system. Invariant theory of finite groups suggests that since the system is invariant there exists a set of invariant equations which have the same set of common zeros [62]. Furthermore these invariant equations can be written as polynomials in a finite generating set of the polynomial invariants [18]. The idea is then to solve for the value of these generators, with the hope that this computation is more feasible than the direct computation. There are two main problems with this plan. First, the symbolic methods for performing this "symmetrization" and "rewriting" rely on Gröbner bases and so are quickly computationally intractable. Second, the set of generating invariants for the action on the variables x_i, X_i, y_i, Y_i is complicated. If we consider only the action on the variables x_i, y_i, then a generating set is simple enough, indeed one may take the elementary symmetric polynomials $e_1^{(x)}, \dots, e_M^{(x)}$ in the variables $x_1, \dots, x_M$ and the

elementary symmetric polynomials $e_1^{(y)}, \dots, e_N^{(y)}$ in the variables $y_1, \dots, y_N$, given by $e_k^{(x)} := \sum_{I\subseteq[M],|I|=k} \prod_{i\in I} x_i$ and $e_k^{(y)} := \sum_{I\subseteq[N],|I|=k} \prod_{i\in I} y_i$, respectively.

We take an indirect approach inpired by the methodology utilized by Faugère and Svartz towards solving for the (rigidly rotating) configurations of vortices of a single charge [22]. The first step is to construct a set of invariant equations, written in terms of invariants in the variables x_i, X_i, y_i, Y_i, whose set of common zeros includes the solutions to System (6) (i.e. those common zeros of the conjugate variable system such that $X_i = \overline{x_i}$ and $Y_i = \overline{y_i}$). From these, we then deduce symmetric equations in the x_i, y_i whose set of common zeros includes the solutions to System (6). The rewriting is done at the same time. The section ends with an explanation of our solution procedure.

3.1. **Invariant equations.** In this section we introduce some invariant equations that are satisfied by the solutions to the vortex problem.

To start, we provide a useful compact form of the conjugate system. We set $P(z) = \prod_{i=1}^{M}(z - x_i)$ and $Q(z) = \prod_{i=1}^{N}(z - y_i)$. We have the following Lemma.

Lemma 3.1. *The system* $\{E_i^{(x)}, \bar{E}_i^{(x)}, E_j^{(y)}, \bar{E}_j^{(y)} \mid i = 1, \dots, M, j = 1 \dots N\}$ *is equivalent to:*

$$(7)\quad \begin{cases} X_i = -\dfrac{P''(x_i)}{2P'(x_i)} + \dfrac{Q'(x_i)}{Q(x_i)}, \quad x_i = -\dfrac{P''(X_i)}{2P'(X_i)} + \dfrac{Q'(X_i)}{Q(X_i)}, \quad i = 1, \dots M, \\ Y_i = -\dfrac{Q''(y_i)}{2Q'(y_i)} + \dfrac{P'(y_i)}{P(y_i)}, \quad y_i = -\dfrac{Q''(Y_i)}{2Q'(Y_i)} + \dfrac{P'(Y_i)}{P(Y_i)}, \quad i = 1, \dots N. \end{cases}$$

Proof. The proof of [22, Lemma 1] shows that $\sum_{\substack{j=1\\ j\neq i}}^{M} \frac{1}{x_i - x_j} = \frac{P''(x_i)}{2P'(x_i)}$. Combining with $\frac{Q'(z)}{Q(z)} = \sum_{j=1}^{N} \frac{1}{z-y_j}$ we get that equation $E_i^{(x)}$ can be rewritten as $X_i = -\frac{P''(x_i)}{2P'(x_i)} + \frac{Q'(x_i)}{Q(x_i)}$. Similar computations hold for the other equations. □

We denote by $s_k^{(x)}$ the Newton sum $s_k^{(x)} = \sum_{i=1}^{M} x_i^k$, and we define $r_k^{(x)} = \sum_{i=1}^{M} x_i^k X_i$. Similarly, we denote $s_k^{(y)} = \sum_{i=1}^{M} y_i^k$, and $r_k^{(y)} = \sum_{i=1}^{M} y_i^k Y_i$.

Theorem 3.2. *For every* $k \geq 0$*, the solutions to System* (6) *satisfy the equation*

$$r_k{}^{(x)} + r_k^{(y)} = \\ -\frac{1}{2}\left(\sum_{i=0}^{k-1} s_i^{(x)} s_{k-i-1}^{(x)}\right) + \frac{k}{2} s_{k-1}^{(x)} - \frac{1}{2}\left(\sum_{i=0}^{k-1} s_i^{(y)} s_{k-i-1}^{(y)}\right) + \frac{k}{2} s_{k-1}^{(y)} + \left(\sum_{i=0}^{k-1} s_i^{(x)} s_{k-i-1}^{(y)}\right).$$

Proof. We have

$$(8)\qquad r_k^{(x)} = \sum_{i=1}^{M} x_i^k X_i = -\sum_{i=1}^{M} \frac{x_i^k P''(x_i)}{2P'(x_i)} + \sum_{i=1}^{M} \frac{x_i^k Q'(x_i)}{Q(x_i)}.$$

By the proof of [22, Theorem 4] we have $-\sum_{i=1}^{M} \frac{x_i^k P''(x_i)}{2P'(x_i)} = -\frac{1}{2}\left(\sum_{i=0}^{k-1} s_i^{(x)} s_{k-i-1}^{(x)}\right) + \frac{k}{2} s_{k-1}^{(x)}$. As a result,

$$r_k^{(x)} = -\frac{1}{2}\left(\sum_{i=0}^{k-1} s_i^{(x)} s_{k-i-1}^{(x)}\right) + \frac{k}{2} s_{k-1}^{(x)} + \sum_{i=1}^{M}\sum_{j=1}^{N} \frac{x_i^k}{x_i - y_j}. \tag{9}$$

Similarly we have

$$r_k^{(y)} = -\frac{1}{2}\left(\sum_{i=0}^{k-1} s_i^{(y)} s_{k-i-1}^{(y)}\right) + \frac{k}{2} s_{k-1}^{(y)} + \sum_{i=1}^{M}\sum_{j=1}^{N} \frac{-y_j^k}{x_i - y_j}. \tag{10}$$

If we sum Equation (9) and Equation (10) we obtain

(11)

$$r_k{}^{(x)} + r_k^{(y)} = \\ -\frac{1}{2}\left(\sum_{i=0}^{k-1} s_i^{(x)} s_{k-i-1}^{(x)}\right) + \frac{k}{2} s_{k-1}^{(x)} - \frac{1}{2}\left(\sum_{i=0}^{k-1} s_i^{(y)} s_{k-i-1}^{(y)}\right) + \frac{k}{2} s_{k-1}^{(y)} + \sum_{i=1}^{M}\sum_{j=1}^{N} \frac{x_i^k - y_j^k}{x_i - y_j}.$$

Let us assume $k \geq 1$. We have $\frac{x_i^k - y_j^k}{x_i - y_j} = \sum_{m=0}^{k-1} x_i^m y_j^{k-m-1}$. It follows that

$$\sum_{i=1}^{M}\sum_{j=1}^{N} \frac{x_i^k - y_j^k}{x_i - y_j} = \sum_{i=1}^{M}\sum_{j=1}^{N}\sum_{m=0}^{k-1} x_i^m y_j^{k-m-1} = \sum_{m=0}^{k-1} s_m^{(x)} s_{k-m-1}^{(y)}. \tag{12}$$

Therefore, for $k \geq 1$, the statement follows immediately from Equation (11) and Equation (12).

Finally, we consider the case $k = 0$. We have

$$r_0^{(x)} = \sum_{i=1}^{M} X_i = -\sum_{i=1}^{M}\sum_{\substack{j=1 \\ j\neq 1}}^{M} \frac{1}{x_i - x_j} + \sum_{i=1}^{N}\sum_{j=1}^{M} \frac{1}{x_i - y_j} \tag{13}$$

$$= -\sum_{\substack{i,j=1 \\ i<j}}^{M} \frac{1}{x_i - x_j} - \sum_{\substack{i,j=1 \\ i<j}}^{M} \frac{1}{x_j - x_i} + \sum_{i=1}^{N}\sum_{j=1}^{M} \frac{1}{x_i - y_j} = \sum_{i=1}^{N}\sum_{j=1}^{M} \frac{1}{x_i - y_j}, \tag{14}$$

$$r_0^{(y)} = \sum_{i=1}^{N}\sum_{j=1}^{M} \frac{1}{y_j - x_i}, \tag{15}$$

and therefore $r_0^{(x)} + r_0^{(y)} = 0$ as desired. □

3.2. **Equations in the elementary symmetric functions.** In Theorem 3.2 we introduced a set of invariant equations to describe the vortex problem. For practical uses, the presence of $r_k^{(x)}$ and $r_k^{(y)}$ in these equations produces two disadvantages:

(1) they involve both the variables x_i's, y_j's and their conjugates X_i's, Y_j's,
(2) there is no easy formula to express $r_k^{(x)}$ in terms of the elementary symmetric functions in the x_i's and X_i's.

We remind the reader that, on the other hand, there exist well known formulas to express the Newton sums $s_k^{(x)}$'s in terms of the elementary symmetric functions $e_k^{(x)}$'s. In this section we obtain a new set of invariant equations for the vortex problem that avoid these issues.

Given a polynomial $F \in K[e_1^{(x)}, \dots e_M^{(x)}, e_1^{(y)} \dots e_N^{(y)}][z]$ in the symmetric polynomials $e_i^{(x)}$'s and $e_i^{(y)}$'s and in the extra variable z, we wish to express in a compact way the sum $\sum_{i=1}^M F(x_i) \pm \sum_{j=1}^N F(y_j)$. To do so, we consider the transformations $\mathscr{S}^+$ and $\mathscr{S}^-$ defined by

$$\begin{array}{rccc} \mathscr{S}^+ : & K[e_1^{(x)}, \dots e_M^{(x)}, e_1^{(y)} \dots e_N^{(y)}][z] & \to & K[e_1^{(x)}, \dots e_M^{(x)}, e_1^{(y)} \dots e_N^{(y)}] \\ & \sum a_k z^k & \mapsto & \sum a_k (s_k^{(x)} + s_k^{(y)}), \end{array}$$

and

$$\begin{array}{rccc} \mathscr{S}^- : & K[e_1^{(x)}, \dots e_M^{(x)}, e_1^{(y)} \dots e_N^{(y)}][z] & \to & K[e_1^{(x)}, \dots e_M^{(x)}, e_1^{(y)} \dots e_N^{(y)}] \\ & \sum a_k z^k & \mapsto & \sum a_k (s_k^{(x)} - s_k^{(y)}), \end{array}$$

where the a_k's are polynomials not involving the variable z. In other words, $\mathscr{S}^\pm$ acts by expanding F in the variable z and then replacing the power z^k with the expression $(s_k^{(x)} \pm s_k^{(y)})$, which, we remind, can be expressed in terms of the symmetric polynomials $e_i^{(x)}$'s and $e_i^{(y)}$'s.

Let $F, G \in K[e_1^{(x)}, \dots e_M^{(x)}, e_1^{(y)} \dots e_N^{(y)}][z]$ be two polynomials, and write them as $F = \sum f_k z^k$ and $G = \sum g_k z^k$. Then, their sum $F + G$ can be written as $F + G = \sum (f_k + g_k) z^k$. It follows that $\mathscr{S}^\pm(F + G) = \mathscr{S}^\pm(F) + \mathscr{S}^\pm(G)$. Similarly, given $F \in K[e_1^{(x)}, \dots e_M^{(x)}, e_1^{(y)} \dots e_N^{(y)}][z]$ and a polynomial $h \in K[e_1^{(x)}, \dots e_M^{(x)}, e_1^{(y)} \dots e_N^{(y)}]$ not involving the variable z, we have $\mathscr{S}^\pm(hF) = h\mathscr{S}^\pm(G)$. However, in general, for $F, G \in K[e_1^{(x)}, \dots e_M^{(x)}, e_1^{(y)} \dots e_N^{(y)}][z]$, we have $\mathscr{S}^\pm(FG) \neq \mathscr{S}^\pm(F)\mathscr{S}^\pm(G)$. These properties sum up to say, in the language of commutative algebra, that $\mathscr{S}^+$ and $\mathscr{S}^+$ are morphisms of $K[e_1^{(x)}, \dots e_M^{(x)}, e_1^{(y)} \dots e_N^{(y)}]$-modules, but not homorphisms of rings. As mentioned above, the transformations $\mathscr{S}^+$ and $\mathscr{S}^-$ allow to write in a convenient way sums of the type $\sum_{i=1}^M F(x_i) \pm \sum_{j=1}^N F(y_j)$.

Lemma 3.3. *For every $F \in K[e_1^{(x)}, \dots e_M^{(x)}, e_1^{(y)} \dots e_N^{(y)}][z]$ we have*

$$\mathscr{S}^\pm(F) = \sum_{i=1}^M F(x_i) \pm \sum_{j=1}^N F(y_j).$$

Proof. We write $F(z) = \sum_k a_k z^k$. We have

$$\mathscr{S}^{\pm}(F) = \sum_k a_k s_k^{(x)} \pm \sum_k a_k s_k^{(y)} = \sum_k \sum_{i=1}^{M} a_k x_i^k \pm \sum_k \sum_{j=1}^{N} a_k y_j^k$$
$$= \sum_{i=1}^{M} \sum_k a_k x_i^k \pm \sum_{j=1}^{N} \sum_k a_k y_j^k = \sum_{i=1}^{M} F(x_i) \pm \sum_{j=1}^{N} F(y_j). \tag{16}$$

□

Corollary 3.4. *For every $F \in K[e_1^{(x)}, \dots e_M^{(x)}, e_1^{(y)} \dots e_N^{(y)}][z]$ we have $\mathscr{S}^{\pm}(FPQ) = 0$.*

Proof. We have $\mathscr{S}^{\pm}(FPQ) = \sum_{i=1}^{M} F(x_i)P(x_i)Q(x_i) \pm \sum_{j=1}^{N} F(y_j)Q(y_j)P(y_j) = 0$, since $P(x_i) = Q(y_j) = 0$ for every $i = 1, \dots, M$ and $j = 1, \dots, N$. □

We are now ready to write expressions for $S_k^{(x)}$, $S_k^{(y)}$, $R_k^{(x)}$ and $R_k^{(y)}$ in terms of $\mathscr{S}^+$ and $\mathscr{S}^-$.

Let D be the resultant of PQ and $(PQ)'$. By definition the *resultant of the polynomials PQ and $(PQ)'$ in one variable z* is a polynomial in their coefficients that vanishes if and only if PQ and $(PQ)'$ have a common root. In particular, it is an element of $K[e_1^{(x)}, \dots e_M^{(x)}, e_1^{(y)} \dots e_N^{(y)}]$, and it can be explicitly computed as the determinant of the Sylvester matrix.

Remark 3.5. The resultant of PQ and $(PQ)'$ is the expression in terms of the elementary symmetric polynomials of the discriminant introduced in Section 2. Indeed, PQ and $(PQ)'$ have a common root if and only if PQ has a double root, which happens only if two among $x_1, \dots, x_M, y_1, \dots, y_N$ coincide.

The discriminant D also satisfies the equation

$$B(z)P(z)Q(z) + C(z)(P(z)Q(z))'$$
$$= B(z)P(z)Q(z) + C(z)(P'(z)Q(z) + P(z)Q'(z)) = D, \tag{17}$$

for some $B, C \in K[e_1^{(x)}, \dots e_M^{(x)}, e_1^{(y)} \dots e_N^{(y)}][z]$.

We then have

$$S_k^{(x)} = \sum_{i=1}^{M} X_i^k = \sum_{i=1}^{M} \left(\frac{-P''(x_i)Q(x_i) + 2P'(x_i)Q'(x_i)}{2P'(x_i)Q(x_i)} \right)^k. \tag{18}$$

Denote

$$A(z) := \frac{1}{2} C(z)(-P''(z)Q(z) + 2P'(z)Q'(z) - P(z)Q''(z)). \tag{19}$$

We have

$$S_k^{(x)} = \sum_{i=1}^{M} \left(\frac{A(x_i)}{C(x_i)P'(x_i)Q(x_i)} \right)^k = \sum_{i=1}^{M} \left(\frac{A(x_i)}{C(x_i)(P'(x_i)Q(x_i) + P(x_i)Q'(x_i))} \right)^k, \tag{20}$$

where we are using on both numerator and denominator the fact that $P(x_i) = 0$ for $i = 1, \dots, M$.

Similarly, for $S^{(y)}$ we get the expression

(21)
$$S_k^{(y)} = \sum_{j=1}^{N} \left(\frac{A(y_j)}{C(y_j)P(y_j)Q'(y_j)} \right)^k = \sum_{j=1}^{N} \left(\frac{A(y_j)}{C(y_j)(P'(y_j)Q(y_j) + P(y_j)Q'(y_j))} \right)^k.$$

So, now

(22)
$$\begin{aligned} S_k^{(x)} \pm S_k^{(y)} &= \sum_{i=1}^{M} \left(\frac{A(x_i)}{D - B(x_i)P(x_i)Q(x_i)} \right)^k \pm \sum_{j=1}^{N} \left(\frac{A(y_j)}{D - B(y_j)P(y_j)Q(y_j)} \right)^k \\ &= \sum_{i=1}^{M} \left(\frac{A(x_i)}{D} \right)^k \pm \sum_{j=1}^{N} \left(\frac{A(y_j)}{D} \right)^k = \frac{1}{D^k} \left(\sum_{i=1}^{M} A(x_i)^k \pm \sum_{j=1}^{N} A(y_j)^k \right) \\ &= \frac{1}{D^k} \mathscr{S}^{\pm}(A^k(z)). \end{aligned}$$

The same computation for $R_k^{(x)} + R_k^{(y)}$ yields

$$R_k^{(x)} + R_k^{(y)} = \frac{1}{D^k} \left(\sum_{i=1}^{M} x_i A(x_i)^k + \sum_{j=1}^{N} y_j A(y_j)^k \right) = \frac{1}{D^k} \mathscr{S}^{+}(zA^k(z)).$$

We are now ready to state the main theorem of this section.

Theorem 3.6. *The solutions to the vortex problem satisfy, for every $k \geq 0$,*

$$\frac{1}{D} \mathscr{S}^{+}(zA^k(z)) = -\frac{1}{2} \sum_{i=0}^{k-1} \left(\mathscr{S}^{-}(A^i(z)) \right) \left(\mathscr{S}^{-}(A^{k-i-1}(z)) \right) + \frac{k}{2} \mathscr{S}^{+}(A^{k-1}(z)).$$

Proof. We rearrange the conjugate equation of Theorem 3.2.

$$R_k^{(x)} + R_k^{(y)} = -\frac{1}{2} \sum_{i=0}^{k-1} (S_i^{(x)} S_{k-i-1}^{(x)} + S_i^{(y)} S_{k-i-1}^{(y)}) + \sum_{i=0}^{k-1} S_i^{(x)} S_{k-i-1}^{(y)} + \frac{k}{2} (S_{k-1}^{(y)} + S_{k-1}^{(x)}). \tag{23}$$

We can also write

$$\begin{aligned} \sum_{i=0}^{k-1} S_i^{(x)} S_{k-i-1}^{(y)} &= \frac{1}{2} \left(\sum_{i=0}^{k-1} S_i^{(x)} S_{k-i-1}^{(y)} + \sum_{i=0}^{k-1} S_i^{(x)} S_{k-i-1}^{(y)} \right) = \\ &\frac{1}{2} \left(\sum_{i=0}^{k-1} S_i^{(x)} S_{k-i-1}^{(y)} + \sum_{i=0}^{k-1} S_{k-i-1}^{(x)} S_i^{(y)} \right) = \frac{1}{2} \sum_{i=0}^{k-1} (S_i^{(x)} S_{k-i-1}^{(y)} + S_{k-i-1}^{(x)} S_i^{(y)}). \end{aligned}$$

This allows to rewrite the Equation (23) as

$$R_k^{(x)} + R_k^{(y)} = -\frac{1}{2} \sum_{i=0}^{k-1} (S_i^{(x)} S_{k-i-1}^{(x)} + S_i^{(y)} S_{k-i-1}^{(y)} - S_i^{(x)} S_{k-i-1}^{(y)} - S_{k-i-1}^{(x)} S_i^{(y)}) + \frac{k}{2} (S_{k-1}^{(y)} + S_{k-1}^{(x)}).$$

We have $R_k^{(x)} + R_k^{(y)} = \frac{1}{D^k}\mathscr{S}^+(zA^k(z))$ and $S_{k-1}^{(x)} + S_{k-1}^{(y)} = \frac{1}{D^{k-1}}\mathscr{S}^+(A^{k-1}(z))$. Moreover we have

$$\begin{aligned} S_i^{(x)}S_{k-i-1}^{(x)} + S_i^{(y)}S_{k-i-1}^{(y)} - S_i^{(x)}S_{k-i-1}^{(y)} - S_{k-i-1}^{(x)}S_i^{(y)} &= (S_i^{(x)} - S_i^{(y)})(S_{k-i-1}^{(x)} - S_{k-i-1}^{(y)}) \\ &= \left(\frac{1}{D^i}\mathscr{S}^-(A^i(z))\right)\left(\frac{1}{D^{k-i-1}}\mathscr{S}^-(A^{k-i-1}(z))\right). \end{aligned}$$

Equation (23) now can be written as

(24)

$$\begin{aligned} &\frac{1}{D^k}\mathscr{S}^+(zA^k(z)) \\ &\qquad = -\frac{1}{2D^{k-1}}\sum_{i=0}^{k-1}\left(\left(\mathscr{S}^-(A^i(z))\right)\left(\mathscr{S}^-(A^{k-i-1}(z))\right)\right) + \frac{k}{2D^{k-1}}(\mathscr{S}^+(A^{k-1}(z))), \end{aligned}$$

and the statement follows at once. □

Remark 3.7. For $k = 0$ it reduces to $e_1^{(x)} + e_1^{(y)} = 0$, for $k = 1$ it reduces to $0 = 0$.

3.3. **From solutions to the invariant system to solutions of (6).** In this section we explain how to obtain solutions for the System (6) using the symmetric system.

The first step will be to solve the invariant system obtained in Theorem 3.6. In this case we will be aiming for complete, exact solutions. The main idea will be for each $k \geq 0$ to write

$$h_k := \frac{1}{D}\mathscr{S}^+(zA^k(z)) + \frac{1}{2}\sum_{i=0}^{k-1}\left(\mathscr{S}^-(A^i(z))\right)\left(\mathscr{S}^-(A^{k-i-1}(z))\right) - \frac{k}{2}\mathscr{S}^+(A^{k-1}(z)).$$

By construction the h_k's are polynomial functions in the elementary symmetric polynomials $e_1^{(x)}, \ldots, e_M^{(x)}$ and $e_1^{(y)}, \ldots, e_N^{(y)}$. By Remark 3.7, we have $h_0 = e_1^{(x)} + e_1^{(y)}$ and $h_1 = 0$. As the polynomial functions $e_1^{(x)}, \ldots, e_M^{(x)}$ and $e_1^{(y)}, \ldots, e_N^{(y)}$ are algebraically independent, we can think of them as coordinate functions on $\mathbb{C}^{M+N}$. Our first step is then to find all points p of $\mathbb{C}^{M+N}$ which satisfy $h_k(p) = 0$ for all k. As polynomial rings in finitely many variables are Noetherian, we know that there exists $K \geq 0$ such that the set of common zeros of $h_0, \ldots, h_K$ coincides with the set of common zeros of all h_k's. Unfortunately, this finiteness result is not constructive, and it is very hard to determine a priori how many h_k's are sufficient. Furthermore, the formulas for the h_k's are rather complicated and each addition makes the symbolic computation less likely to be tractable. Accordingly we make a choice to consider only $h_0, h_2, \ldots, h_{M+N-1}$. This ensures that the number of equations is the same as the number of variables after eliminating $e_1^{(y)}$ via the relation $e_1^{(x)} + e_1^{(y)} = 0$. The set of common zeros of these functions is potentially bigger than the set of common zeros of all the h_k's, but we know this set will include the set of solutions to the System (6).

Proposition 3.8. *Equip $K[e_1^{(x)}, \ldots, e_M^{(x)}, e_1^{(y)}, \ldots, e_N^{(y)}]$ with the structure of a graded ring by declaring $e_1^{(x)}$ and $e_j^{(y)}$ to have degree i and j, respectfully. Then, for each $k \geq 0$ equation h_k is homogeneous of degree $(k-1)\left(\binom{M}{2} + \binom{N}{2} + 2MN - 1\right)$.*

Proof. As noted in the proof of Theorem 3.6, equation (24) is simply a rewriting of the conjugate of the equation in Theorem 3.2. As this equation is homogeneous of degree $k-1$ in the variables $x_1, \ldots, x_M, y_1, \ldots, y_N$, the conjugate is homogenous of degree $1-k$ (indeed, Equations $E_i^{(x)}$ and $E_i^{(x)}$ express X_i and Y_i as homogeneous rational functions of degree -1 in the variables $x_1, \ldots, x_M, y_1, \ldots, y_N$). Next, we note that the discriminant

$$D = \prod_{i \neq j}(x_i - x_j)(-1)^{MN} \prod_{i,j}(x_i - y_j) \prod_{i \neq j}(y_i - y_j)$$

is homogeneous of degree $\binom{M}{2} + \binom{N}{2} + 2MN$ in the variables $x_1, \ldots, x_M, y_1, \ldots, y_N$. It follows that the equation h_k is homogeneous of degree $(k-1)\left(\binom{M}{2} + \binom{N}{2} + 2MN - 1\right)$ in the variables $x_1, \ldots, x_M, y_1, \ldots, y_N$. The conclusion then follows since h_k is invariant and the grading in the statement of the proposition is the grading obtained by taking the degree of the elementary symmetric polynomials in the variables $x_1, \ldots, x_M, y_1, \ldots, y_N$. □

Remark 3.9. The fact that the polynomials h_k are homogeneous means that if $(e_1^{(x)}, \ldots, e_M^{(x)}, e_1^{(y)}, \ldots, e_N^{(y)})$ is a common zero, then so is $(te_1^{(x)}, \ldots, t^M e_M^{(x)}, te_1^{(y)}, \ldots, t^N e_N^{(y)})$ for every $t \in \mathbb{C}$. Equivalently, if $(x_1, \ldots, x_M, y_1, \ldots, y_N)$ is a solution, so is $(tx_1, \ldots, tx_M, ty_1, \ldots, ty_N)$ for every $t \in \mathbb{C}$. This is not surprising. The action of the multiplicative group of complex numbers with modulus 1 on the solutions of Equations (6) implies that for every solution $(x_1, \ldots, x_M, y_1, \ldots, y_N)$ the set $\{(tx_1, \ldots, tx_M, ty_1, \ldots, ty_N) \mid t \in \mathbb{C} \text{ and } |t| = 1\}$ is contained in the set of solutions of Equations (6) and so in the common zeroes of the h_k's. But as the h_k's are polynomials, their common zeroes must contain the Zariski closure of this set, namely $\{(tx_1, \ldots, tx_M, ty_1, \ldots, ty_N) \mid t \in \mathbb{C}\}$.

Question 1. *Are the sets of common zeros of System (6) and the symmetric system from Theorem 3.6 finite up to symmetry?*

Zero-dimensional common zero sets of polynomials are finite, meaning that we could potentially list all solutions. With this in mind, we break down the problem into subclasses by dehomogenizing. Specifically, choosing an order on the variables, say starting with $e_1^{(x)}$, we divide the system into two cases, when $e_1^{(x)} = 0$ and when $e_1^{(x)} \neq 0$. By Remark 3.9 if there is a solution with $e_1^{(x)} \neq 0$, then up to multiplying by a complex number we can assume that $e_1^{(x)} = 1$. Thus we add the equation $e_1^{(x)} = 1$ to the subsystem. Next we consider the case where $e_1^{(x)}$ is zero. Setting a variable to zero does not break the homogeneity and so we can again dehomogenize by setting the second variable to 1, say $e_2^{(x)} = 1$. We continue like this until we run out of variables or the equations become trivial.

For every solution in the elementary symmetric polynomials we find one corresponding solution in the x_i's and y_j's. This is done by solving the system obtained by plugging the solution in the $e_i^{(x)}$'s and $e_i^{(y)}$'s in the equations defining the elementary symmetric polynomials $e_i^{(x)} = \sum_{j_1 < \ldots < j_i} x_{j_1} \cdot \ldots \cdot x_{j_i}$ and $e_i^{(y)} = \sum_{j_1 < \ldots < j_i} y_{j_1} \cdot \ldots \cdot y_{j_i}$.

What we need to do next is on the one hand to remove the arbitrary choices we made when dehomogenizing (for example assuming $e_1^{(x)} = 1$), and on the other hand

check if the common zero of the h_k's we obtained is a solution of the original System (6). We do both at the same time. For every solution in the x_i's and y_j's, we are looking for $\lambda \in \mathbb{C}$ such that $\lambda x_1, \ldots, \lambda y_N$ satisfy system (6). Since we can scale by any complex number of modulus 1, we can restrict this search to λ real and positive. Supposing $x_i \neq 0$, we use the ith equation of system (6) rewritten as

$$\lambda^2 = \frac{1}{\overline{x_i}} \left(-\sum_{\substack{j \neq i \\ j=1}}^{M} \frac{1}{x_i - x_j} + \sum_{j=1}^{N} \frac{1}{x_i - y_j} \right). \tag{25}$$

This allows us to determine the value which could work. We use the remaining equations of system (6) to check if this works for all.

Summary of solution procedure:
We start with the equations $h_0, h_2, \ldots, h_{M+N-1}, hD - 1$.
For i from 1 to M:

(1) We dehomogenize the system by imposing the extra conditions $e_1^{(x)} = \ldots = e_{i-1}^{(x)} = 0$, $e_i^{(x)} = 1$.
(2) We find the (finitely many) solutions to the subsystem obtained in Step (1), for example using Maple PolynomialSystem function.
(3) For each solution in the elementary symmetric polynomials, we find one corresponding solution in the x_i's and y_j's by solving the polynomial systems obtained by substituting each solution in the definition of the elementary polynomials as described above.
(4) For every solution in the x_i's and y_j's, we check wether $\lambda x_1, \ldots, \lambda y_N$ satisfy system (6) for some $\lambda > 0$.

3.4. **Example of equations obtained for small cases.** In this section we give the equations obtained by applying the procedure described in the case $M = 1$, $N = 2$ and explain that the size of the equations get out of hand quickly by giving the number of terms in the polynomials given by our formulas.

We start by writing $P(z) = e_0^{(x)} z^2 - e_1^{(x)} z - e_2^{(x)} = z^2 - e_1^{(x)} z - e_2^{(x)}$ and $Q(z) = e_0^{(y)} z - e_1^{(y)} = z + e_1^{(x)}$. Please notice that, for both P and Q, we have used $e_0^{(x)} = e_0^{(y)} = 1$, and $e_1^{(x)} = -e_1^{(y)}$. This allows us to only work with the two variables $e_1^{(x)}$ and $e_2^{(x)}$.

We then compute the Sylvester matrix of PQ and $(PQ)'$:

$$Sylv = \begin{pmatrix} 1 & 0 & -(e_1^{(x)})^2 + e_2^{(x)} & e_1^{(x)} e_2^{(x)} & 0 \\ 0 & 1 & 0 & -(e_1^{(x)})^2 + e_2^{(x)} & e_1^{(x)} e_2^{(x)} \\ 3 & 0 & -(e_1^{(x)})^2 + e_2^{(x)} & 0 & 0 \\ 0 & 3 & 0 & -(e_1^{(x)})^2 + e_2^{(x)} & 0 \\ 0 & 0 & 3 & 0 & -(e_1^{(x)})^2 + e_2^{(x)} \end{pmatrix}$$

From the Sylvester matrix we can compute the discriminant

$$D = det(Sylv) = -4(e_1^{(x)})^6 + 12(e_1^{(x)})^4 e_2^{(x)} + 15(e_1^{(x)})^2(e_2^{(x)})^2 + 4(e_2^{(x)})^3 = ((e_1^{(x)})^2 - 4e_2^{(y)})((e_1^{(x)})^2 + e_2^{(y)}/2)^2.$$

The polynomial C can also be computed by the Sylvester matrix. Denote by $M = (m_{i,j})$ the adjoint matrix, we have

$$C = m_{5,5} + zm_{5,4} + z^2 m_{5,3} = z^2(-6(e_1^{(x)})^2 + 6e_2^{(x)}) - 9ze_1^{(x)}e_2^{(x)} + 4((e_1^{(x)})^2 - e_2^{(x)})^2.$$

We can now use Equation (19), and write

$$A = \frac{1}{2}(z^2(-6(e_1^{(x)})^2 + 6e_2^{(x)}) - 9ze_1^{(x)}e_2^{(x)} + 4((e_1^{(x)})^2 - e_2^{(x)})^2)(2z - 4e_1^{(x)}).$$

Finally, we can write the equation h_2. Please note that, by Corollary 3.4, we are allowed to replace A with its remainder modulo PQ. We obtain

$$h_2 = -16(e_1^{(x)})^1 1 - 4(e_1^{(x)})^9 e_2^{(y)} + 356(e_1^{(x)})^7(e_2^{(y)})^2 - 209(e_1^{(x)})^5(e_2^{(y)})^3 - 473(e_1^{(x)})^3(e_2^{(y)})^4 - 140e_1^{(x)}(e_2^{(y)})^5$$

As a further optimization we can apply before solving the equations, we divide h_2 by the highest possible power of the factors of the discriminant. We finally get the system of equations:

$$(26) \quad \begin{cases} h_2' = -16(e_1^{(x)})^5 - 52(e_1^{(x)})^3 e_2^{(y)} + 140e_1^{(x)}(e_2^{(y)})^2 = 0 \\ hD = h(-4(e_1^{(x)})^6 + 12(e_1^{(x)})^4 e_2^{(y)} + 15(e_1^{(x)})^2(e_2^{(y)})^2 + 4(e_2^{(y)})^3) = 1 \end{cases}$$

To solve the equations, we consider two cases.

- Case 1, $e_1^{(x)} = 1$. By replacing $e_1^{(x)}$ with 1 in the equations we get two solutions.
  First solution: $h = -\frac{100}{81}$, $e_1^{(x)} = 1$, $e_2^{(y)} = -\frac{1}{5}$.
  Second solution: $h = -\frac{98}{81}$, $e_1^{(x)} = 1$, $e_2^{(y)} = -\frac{4}{7}$.
- Case 2, $e_1^{(x)} = 0$, $e_2^{(y)} = 0$. By replacing in the system we get $h = 0$ and the trivial equation, which means that $e_1^{(x)} = 0$, $e_2^{(y)} = 0$ is again a solution.
  Third solution: $h = 0$, $e_1^{(x)} = 0$, $e_2^{(y)} = 0$.

Once we have obtained the solutions in the elementary symmetric polynomials, we translate them into solution in the x_1, y_1, y_2 variables. This is done by plugging the solutions obtained into the definition of the elementary symmetric powers.

$$\begin{cases} e_1^{(x)} = x_1, \\ e_1^{(y)} = y_1 + y_2, \\ e_2^{(y)} = y_1 y_2. \end{cases}$$

We now get three solutions, namely

- Solution 1: $x_1 = 1,\ y_1 \approx -1.17,\ y_2 \approx 0.17$;

		$M=2$ $N=1$	$M=3$ $N=1$	$M=4$ $N=1$	$M=5$ $N=1$	$M=2$ $N=2$	$M=3$ $N=2$	$M=3$ $N=3$
	n of variables	2	3	4	5	3	4	5
h_2	degree	5	10	14	24	10	14	19
h_2	n monomials	3	15	71	575	16	124	912
h_3	degree	-	6	10	37	6	10	37
h_3	n monomials	-	6	36	4153	9	49	12132
h_4	degree	-	-	28	42	-	28	37
h_4	n monomials	-	-	419	5708	-	785	12148
h_5	degree	-	-	-	55	-	-	55
h_5	n monomials	-	-	-	20765	-	-	63136

TABLE 1. Degree and number of monomials of the equations for different values of M and N. The numbers refer to the equations after dividing by factors of the discriminant.

- Solution 2: $x_1 = 1,\ y_1 \approx -0.5 - 0.57i,\ y_2 \approx -0.5 + 0.567i$;
- Solution 3: $x_1 = 0,\ y_1 = -i,\ y_2 = i$.

For each one of them, we need to test whether, for some λ, $(\lambda x_1, \lambda y_1, \lambda y_2)$ solve Equation (6). This is easily done: we obtain three linear equations in $|\lambda|^2$ and we have to determine whether they have a common solution. In the case discussed, only the third solution provides a solution to Equation (6), namely for $|\lambda| = \sqrt{2}/2$.

Table 1 compares the degree and number of monomials of the equations we get for different values of M and N. The numbers refer to the equations after dividing by factors of the discriminant, as in Equation (26).

4. Results and Benchmark

In this section, we present the solutions we have found and give details of the computations performed. The invariant equations described in the previous section are extremely long. We first attempted to write them in the software Macaulay2 [27]. This was, however, extremely demanding in terms of processor time and memory requirements. The same operation was far more efficient using the software Maple [1]. One possible reason for this difference, is that Maple does not expand products of polynomial (in our case, the powers of A) unless required to do so.

Classical numerical methods, such as Newton's method, often require some initial guess and lead to one approximate solution. However, there can be multiple solutions to a given system of equations, and there is no guarantee that one will find all of them. Given a system of polynomial equations, we use techniques developed in computational algebraic geometry and commutative algebra to compute *all* solutions.

- Symbolic AG: The most common symbolic method is based on the computation of a Gröbner basis for the system. Gröbner bases provide a systematic way to symbolically find the set of common zeroes of a system of polynomials. Gröbner bases are (typically very long) lists of generators of the system

of polynomial equations with good algebraic properties which can be understood as a multivariate generalization of Gaussian elimination. For more details, see [15].

- Numerical AG: Numerical algebraic geometry methods are based on "homotopy continuation". The system is put in a continuous deformation (a homotopy) to an appropriate "known" start system with similar properties. The solutions of the known system are tracked over $\mathbb{C}$ using homotopy continuation, which provides numerical approximations of all the distinct or isolated complex solutions of the original system, and these can be certified. By running homotopy continuation with appropriate generic homotopy parameter over $\mathbb{C}$, not $\mathbb{R}$, numerical algebraic geometry techniques with probability 1 find all solutions along the path [47]. For details see [10, 61]. Since formulation is important for numerical conditioning, Section 4.1 considers an alternative formulation which is better conditioned.

We attempted to compute the solutions of the vortex problem following both of these approaches. As exact method, we used the function `PolynomialSystem` contained in the package `SolveTools` of the software Maple [1]. We used Bertini [9], an open numerical algebraic geometry software, which contains an implementation of homotopy continuation and numerically solves for all solutions.

Table 2 compares the running time (in seconds) of the two approaches on the invariant system as well as on the systems described in Section 2.1. The computations was performed on a standard office desktop (Intel i3 3.40GHz with 7.7GB ram).

4.1. **Improving the conditioning of the system.** One approach for creating a polynomial system from the rational equations $(\bar{E}_i^{(x)})$, $(\bar{E}_i^{(y)})$, $(E_i^{(x)})$, $(E_i^{(y)})$ is to clear denominators as in Section 2.1. Although this does not add variables, it increases the degrees which negatively impacts the numerical conditioning of the system. An alternative approach to constructing a polynomial system which has improved conditioning at the expense of more variables is to introduce a new variable for each rational term. For example, one introduces $\binom{M}{2}$ new variables $Rx_{i,j}$ equal to the term $\frac{1}{x_i - x_j}$ where $i = 1, \ldots, M$ and $j = i+1, \ldots, M$ yielding the bilinear constraint

$$Rx_{i,j} \cdot (x_i - x_j) = 1. \tag{27}$$

For $j < i$, one has $Rx_{j,i} = -Rx_{i,j}$. After introducing new variables $Ry_{i,j}$, $RX_{i,j}$, $RY_{i,j}$, $Rxy_{i,j}$, and $RXY_{i,j}$ similarly, the equations $(\bar{E}_i^{(x)})$, $(\bar{E}_i^{(y)})$, $(E_i^{(x)})$, $(E_i^{(y)})$ simply reduce to linears. Hence, the only nonlinearity arises from the bilinear constraints for the new variables such as (27). In fact, the resulting system is naturally multihomogeneous so one can employ multihomogeneous regeneration [31, 32] to efficiently solve.

4.2. **List of solutions.** Table 4 contains all the solutions of the system for different values of M and N. For $M = 3, N = 3$ and for $M = 4, N = 2$ the computation of the main component ($e_1^{(x)} = 1$) did not terminate when using Maple, but Bertini was able to solve the corresponding reconditioned systems. Nonetheless, Maple was able to compute all solutions where at least one variable $e_i^{(x)}$ or $e_i^{(y)}$ equals zero. For

Method	$M=2$ $N=1$	$M=2$ $N=2$	$M=3$ $N=1$	$M=3$ $N=2$
Invariants equations with Maple	1.6	2.7	2.2	42.6
Real and imaginary part with Maple (Sec 2.1.1)	0.2	3.8	1.7	ran out of memory
Real and imaginary part with Bertini (Sec 2.1.1)	988	> 10000	> 10000	> 10000
Conjugate variables with Maple (Sec 2.1.2)	0.4	6.5	2.4	ran out of memory
Conjugate variables with Bertini (Sec 2.1.2)	2401	> 10000	> 10000	> 10000
Reconditioned system with Bertini (Sec 4.1)	0.3	8.0	7.8	80.9

TABLE 2. Running time in seconds of the two approaches on the invariant system as well as on the systems described in Subsection 2.1. The first five computations was performed on a standard office desktop (Intel i3 3.40GHz with 7.7GB ram) The Bertini optimized computations were performed with 1 processor for the (2,1) case and 64 processors in parallel for the other cases.

	$M=1$ $N=1$	$M=2$ $N=1$	$M=2$ $N=2$	$M=3$ $N=1$	$M=3$ $N=2$	$M=4$ $N=1$	$M=3$ $N=3$	$M=4$ $N=2$
|sol's|	1	1	2	0	1	0	≥ 2	≥ 1

TABLE 3. Number of solutions found for different values of M and N. For $M=3, N=3$ and for $M=4, N=2$ there may be more solutions.

all other values of M and N in the table 4, the Bertini computation was completed, providing computational proof that no more solutions are present.

5. Connection to the GP PDE Results

Many of the above obtained configurations have been previously identified at the level of the GP equation. In particular, for instance, the vortex dipoles ($M=N=1$) have emerged as the lowest order configuration that destabilizes a planar dark soliton state [40, 44, 45] and have also been obtained experimentally via different techniques [52, 46], enabling the observation of their precessional dynamics. Importantly, in [46], the stationary form of the configuration directly related to the considerations herein, was also experimentally identified. Furthermore, in some of these

$(1,1)$	$x_1 = -\sqrt{2}/2 \approx -0.707$	$y_1 = \sqrt{2}/2 \approx 0.707$
$(2,1)$	$x_1 = -\sqrt{2}/2 \approx -0.707$	$y_1 = 0$
	$x_2 = \sqrt{2}/2 \approx 0.707$	
$(2,2)$	$x_1 = -\sqrt{2}/2 \approx -0.707$	$y_1 = -\sqrt{2}/2i \approx -0.707i$
	$x_2 = \sqrt{2}/2 \approx 0.707$	$y_2 = \sqrt{2}/2i \approx 0.707i$
$(2,2)$	$x_1 = \frac{\sqrt{2+2\sqrt{2\sqrt{2}-2}}}{2} \approx 0.977$	$y_1 = -\frac{\sqrt{2+2\sqrt{2\sqrt{2}-2}}}{2} \approx -0.977$
	$x_2 = -\frac{\sqrt{2-2\sqrt{2\sqrt{2}-2}}}{2} \approx -0.212$	$y_2 = \frac{\sqrt{2-2\sqrt{2\sqrt{2}-2}}}{2} \approx 0.212$
$(3,2)$	$x_1 \approx 0$	$y_1 = \frac{1-\sqrt{3}}{2} \approx -0.366$
	$x_2 = -\sqrt[4]{\frac{3}{4}} \approx -0.930$	$y_2 = \frac{\sqrt{3}-1}{2} \approx 0.366$
	$x_3 = \sqrt[4]{\frac{3}{4}} \approx 0.930$	
$(3,3)$	$x_1 = \sqrt{2}/2 \approx 0.707$	$y_1 = -\sqrt{2}/2 \approx -0.707$
	$x_2 = -\frac{1-i\sqrt{3}}{2\sqrt{2}} \approx -0.354 + 0.612i$	$y_2 = \frac{1+i\sqrt{3}}{2\sqrt{2}} \approx 0.354 + 0.612i$
	$x_3 = -\frac{1+i\sqrt{3}}{2\sqrt{2}} \approx -0.354 - 0.612i$	$y_3 = \frac{1-i\sqrt{3}}{2\sqrt{2}} \approx 0.354 - 0.612i$
$(3,3)$	$x_1 \approx -0.476$	$y_1 \approx 0.476$
	$x_2 \approx 0.162$	$y_2 \approx -0.162$
	$x_3 \approx 1.112$	$y_3 \approx -1.112$
$(4,2)$	$x_1 = -\sqrt{\frac{1-\sqrt{10}}{6}} \approx -0.600i$	$y_1 = -\sqrt{\frac{3-\sqrt{10}}{2}} \approx -0.285i$
	$x_2 = -\sqrt{\frac{13-4\sqrt{10}}{6}} \approx -0.242$	$y_2 = \sqrt{\frac{3-\sqrt{10}}{2}} \approx 0.285i$
	$x_3 = \sqrt{\frac{13-4\sqrt{10}}{6}} \approx 0.242$	
	$x_4 = \sqrt{\frac{1-\sqrt{10}}{6}} \approx 0.600i$	

TABLE 4. List of solutions found. The positions of the positively charged x_i and negatively charged y_i vortices are provided that solve Equations (6).

works [44, 45], it was argued that the aligned configurations of the tripole with $M = 2$, $N = 1$ (which was also observed experimentally in [59]), the aligned quadrupole with $M = 2$, $N = 2$, then the aligned states with $M = 3$, $N = 2$, as well as that with $M = 3$, $N = 3$ (and so on) are all byproducts of subsequent progressive further destabilizations of the dark soliton stripe. That is, for such a stripe [44], each additional destabilization produces a stationary configuration with one additional vortex along the former dark line soliton. This is an intriguing cascade of bifurcations from the stripe which explains the emergence of aligned alternating charge vortex configurations, each with one additional charge with respect to the previous one. Each of these arises through a (supercritical) pitchfork bifurcation which, in turn, justifies that each of these has an additional unstable eigendirection with respect to the previous one. Consequently, the vortex dipole is the most robust among these configurations, bearing no real eigenvalues (and no exponential instabilities), but only an internal, potentially resonant via a Hamiltonian Hopf bifurcation, mode in the

system. Then the tripole would bear one exponentially unstable eigendirection, the aligned quadrupole two such, and so on.

It is important here to highlight that some of the early existence and even stability results on the subject were obtained in the works of [16, 48, 49]. In these works, in addition to some of the aligned configurations, including the dipole and tripole, the first example of a canonical polygon of alternating vortices, namely the quadrupole was identified. It was, in fact, found that this configuration too did not bear any exponential instabilities but could become unstable through an oscillatory instability. The work of [45] offered a more systematic viewpoint on these polygonal configurations (see also [7]). There, it was found that these states too were a result of the destabilization of a dark solitonic stripe, but this time a radial one, the so-called ring dark soliton or RDS configuration (first proposed in the BEC context in [63]). In particular, as soon as this state emerges (in the linear limit of the system) it is degenerate with the vortex quadrupole. Then, its next (further) destabilizing bifurcation gives birth to a vortex hexagon, the subsequent one to a vortex octagon, then to a decagon and so on. All of these lead to canonical polygons involving alternating pairs of vortices, each of which has one more (again) unstable eigendirection to the previous one, i.e., the hexagon is generically unstable due to pairs of eigenvalues emerging as a result of the destabilization of the RDS. Moreover, the method of generating functions was used to illustrate that states with $M = N$, can be used to construct polygons of angle $\phi = \pi/N$ (at a fixed radius) between the alternating charges.

To give a canonical example in the context of configurations considered herein, we briefly refer to the case of the hexagon. In Figure 2, we provide a typical scenario involving the case of $\mu = 2$ and $\Omega = 0.1$. We consider the different layers of approximation, starting with Equation (2), which is the one also tackled via our algebraic techniques. At that level, as is established in [8] (and also found herein) the positions of the vortices are cube roots of unity for both the positive and negative charges, displaced by $\pi/3$ with respect to each other. The radius of the solutions, as shown also in Table 3 (for the complex (3,3) roots) is $\sqrt{2}/2 \approx 0.707$. This radius is given in units of the Thomas-Fermi radius $R_{TF} = \sqrt{2\mu}/\Omega$. As seen in Figure 2, the realistic radius is closer to $0.35R_{TF}$ in the full numerical (PDE) computations. This difference is reflected by the more accurate nature of Equations (4) and (5). It is worthwhile to note that given the equidistant from the origin nature of this configuration as regards the vortices, in this case these two equations [(4) and (5)] yield the same prediction. For both of them, the equilibrium radius is found to be $R^2 = (2\omega_{pr}(0) + R_{TF}^{-2})^{-1}$. For the parameters above, $R = 7.564 = 0.378R_{TF}$; notice that this is very close to the numerical result, the difference being justified by the deviation of the above $\mu = 2$ scenario from the Thomas-Fermi limit of large values of μ. Nevertheless, it is clear that the qualitative picture is accurate in all the effective particle descriptions and that the improved models can yield an even quantitatively accurate characterization. It is relevant to note that the stability results of Figure 2 indicate that this is an unstable configuration due to two nearly identical pairs of real eigenvalues, suggesting an exponential growth of perturbations along the corresponding eigendirections.

All of the above configurations have also been summarized in the compendium of [37] and it is interesting to note that they include *all* the configurations that we

have obtained in the present work *except for* the $M = 4$, $N = 2$ state of Figure 5. It is thus the latter that we now turn our attention to more systematically, as it is unprecedented in earlier both existence and stability studies, to the best of our knowledge. This configuration consists of 4 plus and 2 minus (or vice versa) charged vortices with the inner ones constituting a quadrupole –with slightly unequal distances from the origin along the two axes–, while the last two are aligned with one of the axes and oppositely charged to the rest of the vortices along the same line. A typical example of this configuration was obtained and is shown in Figure 3. Importantly, in this example our numerical observations once again bear some difference in comparison to the prediction of Table 3. In particular, numerically we find the vortices to be located as follows. The +1 charges are located at $x_{1,2} = \pm 0.1875 R_{TF} i$ (along the imaginary axis) and at $x_{3,4} = 0.3875 R_{TF}$, while the -1 charges are at $y_{1,2} = \pm 0.15 R_{TF}$ (cf. with the values in Table 3). The latter four vortices are located on the real axis, although clearly the entire configuration is freely amenable to azimuthal rotations. It is for this reason that we now resort to the progressively more accurate representations of Equations (4) [which accounts for the radial dependence of the vortex precession frequency] and then Equations (5) [which additionally incorporates the effect of the inhomogeneity of the background in the inter-vortex interaction]. The former yields a prediction of $x_{1,2} = \pm 0.158 R_{TF} i$ and $x_{3,4} = \pm 0.331 R_{TF}$ while $y_{1,2} = \pm 0.134 R_{TF}$. Finally, the most accurate available description of Equations (5) leads to the following numbers $x_{1,2} = \pm 0.179 R_{TF} i$, $x_{3,4} = 0.413 R_{TF}$, while $y_{1,2} = \pm 0.154 R_{TF}$. This latter description is the most accurate one –to the best of our knowledge– that is obtained by a particle model, being limited only by the deviation from the Thomas-Fermi limit. That is, the prediction would only be better for larger values of μ. Nevertheless, the conclusion that we reach is that the configuration predicted by the computer algebra techniques is qualitatively consonant with the configuration identified in the full system. Nevertheless, the more elaborate (and more accurate) models such as ultimately that of Equations (5) are needed in order to most adequately capture the quantitative specifics of the vortex locations. In that light, the tools developed herein can be useful in unraveling configurations possibly with quite limited symmetry characteristics which may not be easily identifiable differently. It should also be added that we have explored the dynamical stability of this configuration and have found it to be dynamically unstable, as shown in Figure 3. In particular, as can be observed in the figure, it bears two pairs of real eigenvalues and a complex eigenvalue quartet with nontrivial growth rates. The former lead to an exponential growth along the respective eigendirections, while the latter corresponds to an oscillatory growth due to the complex nature of the eigenvalues.

6. Conclusions & Future Challenges

In the present work, we have made an attempt to bring to bear tools from the theory of Gröbner bases and associated computational algebra to the case of a problem involving stationary configurations of oppositely charged vortices in atomic Bose-Einstein condensates. More specifically, we have started from the corresponding PDE system (of the Gross-Pitaevskii type) and have discussed different layers of reduction approximations characterizing the dynamics of the vortices. The first layer

is a quasi-homogeneous one, the next involves the dependence of the precession frequency of a single vortex on the distance, while the most elaborate one also accounts for the inhomogeneity of the background in affecting inter-vortex interactions. For computational simplicity reasons, we have utilized the simplest one of these descriptions and deduced from its corresponding steady state problem, a set of equations in the elementary symmetric polynomials in the variables. We have brought to bear computational algebra packages that have enabled us, in this adapted formulation, to find *all* possible stationary configurations involving up to 5 vortices of combined positive and negative charges and all stationary configurations involving 6 vortices except for the case of 5 positive and 1 negative charges (or vice versa). Most configurations among these have been already obtained in the literature of BECs, most notably the configurations with high symmetry (axial ones with all the vortices on a line, or polygonal ones with them sitting at the vertices of a canonical polygon). We have discussed in some further detail one of these cases, namely a canonical hexagon, consisting of 3 plus and 3 minus charged vortices. *Nevertheless*, already in the case of 6 charges, we have presented an unprecedented –to the best of our knowledge– configuration, namely one with 4 positive and 2 negative charges (or vice versa). We have studied such a configuration at the level of our different layers of ODE approximation in comparison with computations of the original PDE. In all the cases considered, while admittedly we have utilized (for computational simplicity) the computer algebra package in the simplest setting of Equation (2), we have found that the identified configurations in *all* cases, persist in the full PDE problem. Additionally, we have shown how the more adequate (but at the same time more complex) polynomial equations of the models of Equations (4) and (5) can then facilitate a more accurate capturing of the precise vortex locations in connection with the full PDE problem, providing in this way a more definitive characterization of the states.

We believe that this larger scale program has numerous directions for potential further development. A natural question concerns the limitations of this effort regarding the attempt to seek all the possible configurations with higher numbers of charges. Presently, this task seems somewhat limited by computational capabilities, but it seems reasonably likely that advances in either the algorithmic developments or the computational hardware may be able in the near future to circumvent this issue and offer us an unprecedented ability to obtain *all* stationary vortex configurations of higher numbers of charges. A complementary effort may be developed in the direction of bringing to bear similar algebraic techniques but for the more complex and thus more cumbersome systems, such as those of Equations (4) and especially so Equations (5). Finally, there are numerous additional directions where one can extend present considerations. While a large vein of potential work can be opened by considering three-dimensional settings, we limit our considerations to the 2d case, but involving potentially traveling configurations. There exist works such as those of [35] and more recently [41] which have discussed intriguing algebraic connections including those with the so-called Adler-Moser polynomials (see also references therein). Nevertheless one can envision important, physically relevant variations where the vortices are confined in one direction in the plane, while traveling in the other direction. There, it is conceivable that the nice algebraic structure of the Adler-Moser

polynomials disappears, yet a computer algebra characterization of steadily propagating solutions may well be possible. These different directions are currently under consideration and progress along them will be reported in future publications.

Acknowledgements. Initial work on this project was funded by the John Fell Oxford University Press (OUP) Research Fund. H.A.H. acknowledges support from a Royal Society University Research Fellowship. E.D. and P.T. were supported by the University of Nottingham via a Anne McLaren Fellowship. J.D.H. acknowledges support by the National Science Foundation under Grant No. CCF-1812746. P.G.K. acknowledges useful discussions on the subject with R. Carretero and is based upon work supported by the National Science Foundation under Grant No. PHY-1602994 and DMS-1809074. P.G.K. also acknowledges support from the Leverhulme Trust via a Visiting Fellowship and thanks the Mathematical Institute of the University of Oxford for its hospitality during this work. All authors thank the anonymous referee for their comments, questions and suggestions which have lead to an improved final version.

References

[1] Maple (2017). Maplesoft, a division of Waterloo Maple Inc., Waterloo, Ontario.

[2] C. Aholt, B. Sturmfels, and R. Thomas. A Hilbert scheme in computer vision. *Canad. J. Math*, 65(5):961–988, 2013.

[3] B. Anderson, P. Haljan, C. Regal, D. Feder, L. Collins, C. W. Clark, and E. A. Cornell. Watching dark solitons decay into vortex rings in a Bose–Einstein condensate. *Phys. Rev. Lett.*, 86:2926–2929, Apr 2001.

[4] B. Anderson, P. Haljan, C. E. Wieman, and E. A. Cornell. Vortex precession in Bose–Einstein condensates: Observations with filled and empty cores. *Phys. Rev. Lett.*, 85:2857–2860, Oct 2000.

[5] H. Aref. Vortices and polynomials. *Fluid Dynamics Research*, 39(1):5 – 23, 2007. In memoriam: Professor Isao Imai, 1914-2004.

[6] H. Aref, P. K. Newton, M. A. Stremler, T. Tokieda, and D. L. Vainchtein. Vortex crystals. *Adv. Appl. Mech.*, 39:1–79, 2003.

[7] A. Barry and P. Kevrekidis. Few-particle vortex cluster equilibria in Bose-Einstein condensates: existence and stability. *Journal of Physics A: Mathematical and Theoretical*, 46(44):445001, 2013.

[8] A. M. Barry, F. Hajir, and P. Kevrekidis. Generating functions, polynomials and vortices with alternating signs in Bose–Einstein condensates. *Journal of Physics A: Mathematical and Theoretical*, 48(15):155205, 2015.

[9] D. J. Bates, J. D. Hauenstein, A. J. Sommese, and C. W. Wampler. Bertini: Software for numerical algebraic geometry. Available at bertini.nd.edu with permanent doi: dx.doi.org/10.7274/R0H41PB5.

[10] D. J. Bates, J. D. Hauenstein, A. J. Sommese, and C. W. Wampler. *Numerically solving polynomial systems with Bertini*, volume 25 of *Software, Environments, and Tools*. Society for Industrial and Applied Mathematics (SIAM), Philadelphia, PA, 2013.

[11] W. Bosma, J. Cannon, and C. Playoust. The Magma algebra system. I. The user language. *J. Symbolic Comput.*, 24(3-4):235–265, 1997. Computational algebra and number theory (London, 1993).

[12] A. S. Bradley and B. P. Anderson. Energy spectra of vortex distributions in two-dimensional quantum turbulence. *Phys. Rev. X*, 2:041001, Oct 2012.

[13] V. Bretin, P. Rosenbusch, F. Chevy, G. Shlyapnikov, and J. Dalibard. Quadrupole oscillation of a single-vortex Bose–Einstein condensate: Evidence for kelvin modes. *Phys. Rev. Lett.*, 90:100403, Mar 2003.

[14] B. Buchberger. An algorithm for finding the basis elements of the residue class ring of a zero dimensional polynomial ideal. *J. Symbolic Comput.*, 41(3-4):475–511, 2006. Translated from the 1965 German original by Michael P. Abramson.

[15] D. A. Cox, J. Little, and D. O'Shea. *Ideals, varieties, and algorithms*. Undergraduate Texts in Mathematics. Springer, Cham, fourth edition, 2015. An introduction to computational algebraic geometry and commutative algebra.

[16] L.-C. Crasovan, V. Vekslerchik, V. M. Pérez-García, J. P. Torres, D. Mihalache, and L. Torner. Stable vortex dipoles in nonrotating Bose–Einstein condensates. *Phys. Rev. A*, 68:063609, Dec 2003.

[17] W. Decker, G.-M. Greuel, G. Pfister, and H. Schönemann. SINGULAR 4-1-1 — A computer algebra system for polynomial computations. `http://www.singular.uni-kl.de`, 2018.

[18] H. Derksen and G. Kemper. *Computational invariant theory*, volume 130 of *Encyclopaedia of Mathematical Sciences*. Springer, Heidelberg, enlarged edition, 2015. With two appendices by Vladimir L. Popov, and an addendum by Norbert A'Campo and Popov, Invariant Theory and Algebraic Transformation Groups, VIII.

[19] M. Drton, B. Sturmfels, and S. Sullivant. *Lectures on algebraic statistics*, volume 39. Springer Science & Business Media, 2008.

[20] Z. Dutton, M. Budde, C. Slowe, and L. V. Hau. Observation of quantum shock waves created with ultra- compressed slow light pulses in a Bose–Einstein condensate. *Science*, 293(5530):663–668, 2001.

[21] J.-C. Faugère. A new efficient algorithm for computing Gröbner bases without reduction to zero (F_5). In *Proceedings of the 2002 International Symposium on Symbolic and Algebraic Computation*, pages 75–83. ACM, New York, 2002.

[22] J.-C. Faugère and J. Svartz. Solving polynomial systems globally invariant under an action of the symmetric group and application to the equilibria of N vortices in the plane. In *ISSAC 2012—Proceedings of the 37th International Symposium on Symbolic and Algebraic Computation*, pages 170–178. ACM, New York, 2012.

[23] A. L. Fetter and A. A. Svidzinsky. Vortices in a trapped dilute Bose–Einstein condensate. *Journal of Physics: Condensed Matter*, 13(12):R135, 2001.

[24] D. Freilich, D. Bianchi, A. Kaufman, T. Langin, and D. Hall. Real-time dynamics of single vortex lines and vortex dipoles in a Bose–Einstein condensate. *Science*, 329(5996):1182–1185, 2010.

[25] K. Gatermann. *Computer algebra methods for equivariant dynamical systems*. Springer, 2007.

[26] B. Gertjerenken, P. G. Kevrekidis, R. Carretero-Gonzalez, and B. Anderson. Generating and manipulating quantized vortices on-demand in a Bose–Einstein condensate: A numerical study. *Phys. Rev. A*, 93:023604, Feb 2016.

[27] D. R. Grayson and M. E. Stillman. Macaulay2, a software system for research in algebraic geometry. Available at `http://www.math.uiuc.edu/Macaulay2/`.

[28] A. J. Groszek, D. M. Paganin, K. Helmerson, and T. P. Simula. Motion of vortices in inhomogeneous Bose–Einstein condensates. *Phys. Rev. A*, 97:023617, Feb 2018.

[29] P. Haljan, B. Anderson, I. Coddington, and E. A. Cornell. Use of surface-wave spectroscopy to characterize tilt modes of a vortex in a Bose–Einstein condensate. *Phys. Rev. Lett.*, 86:2922–2925, Apr 2001.

[30] H. A. Harrington, K. L. Ho, T. Thorne, and M. P. Stumpf. Parameter-free model discrimination criterion based on steady-state coplanarity. *Proceedings of the National Academy of Sciences*, 109(39):15746–15751, 2012.

[31] J. D. Hauenstein and J. I. Rodriguez. Multiprojective witness sets and a trace test. *Advances in Geometry*, to appear, 2020.

[32] J. D. Hauenstein, A. J. Sommese, and C. W. Wampler. Regeneration homotopies for solving systems of polynomials. *Math. Comp.*, 80(273):345–377, 2011.

[33] W. R. Inc. Mathematica, Version 11.3. Champaign, IL, 2018.
[34] T. Isoshima, M. Okano, H. Yasuda, K. Kasa, J. Huhtamäki, M. Kumakura, and Y. Takahashi. Spontaneous splitting of a quadruply charged vortex. *Phys. Rev. Lett.*, 99:200403, Nov 2007.
[35] J. B. Kadtke and L. Campbell. Method for finding stationary states of point vortices. *Phys. Rev. A*, 36:4360–4370, Nov 1987.
[36] P. Kevrekidis, W. Wang, R. Carretero-González, D. Frantzeskakis, and S. Xie. Vortex precession dynamics in general radially symmetric potential traps in two-dimensional atomic Bose–Einstein condensates. *Phys. Rev. A*, 96:043612, Oct 2017.
[37] P. G. Kevrekidis, D. J. Frantzeskakis, and R. Carretero-González. *The Defocusing Nonlinear Schrodinger Equation*. Society for Industrial and Applied Mathematics, Philadelphia, PA, 2015.
[38] M. J. Ku, B. Mukherjee, T. Yefsah, and M. W. Zwierlein. Cascade of solitonic excitations in a superfluid fermi gas: From planar solitons to vortex rings and lines. *Phys. Rev. Lett.*, 116:045304, Jan 2016.
[39] R. Laubenbacher and B. Sturmfels. Computer algebra in systems biology. *The American Mathematical Monthly*, 116(10):882–891, 2009.
[40] W. Li, M. Haque, and S. Komineas. Vortex dipole in a trapped two-dimensional Bose–Einstein condensate. *Phys. Rev. A*, 77:053610, May 2008.
[41] Y. Liu and J. Wei. Multi-vortex traveling waves for the Gross–Pitaevskii equation and the Adler–Moser polynomials. 2018.
[42] Y. J. Liu and J. Peddieson. Application of groebner basis methodology to nonlinear mechanics problems. In *International Congress on Mathematical Software*, pages 398–405. Springer, 2014.
[43] E. W. Mayr and A. R. Meyer. The complexity of the word problems for commutative semigroups and polynomial ideals. *Advances in mathematics*, 46(3):305–329, 1982.
[44] S. Middelkamp, P. Kevrekidis, D. Frantzeskakis, R. Carretero-González, and P. Schmelcher. Bifurcations, stability, and dynamics of multiple matter-wave vortex states. *Phys. Rev. A*, 82:013646, Jul 2010.
[45] S. Middelkamp, P. Kevrekidis, D. Frantzeskakis, R. Carretero-González, and P. Schmelcher. Emergence and stability of vortex clusters in Bose–Einstein condensates: A bifurcation approach near the linear limit. *Physica D: Nonlinear Phenomena*, 240(18):1449 – 1459, 2011.
[46] S. Middelkamp, P. Torres, P. Kevrekidis, D. Frantzeskakis, R. Carretero-González, P. Schmelcher, D. Freilich, and D. Hall. Guiding-center dynamics of vortex dipoles in Bose–Einstein condensates. *Phys. Rev. A*, 84:011605, Jul 2011.
[47] A. P. Morgan and A. J. Sommese. Coefficient-parameter polynomial continuation. *Applied Mathematics and Computation*, 29(2):123–160, 1989.
[48] M. Möttönen, S. Virtanen, T. Isoshima, and M. Salomaa. Stationary vortex clusters in nonrotating Bose–Einstein condensates. *Phys. Rev. A*, 71:033626, Mar 2005.
[49] M. Möttönen, S. Virtanen, T. Isoshima, and M. Salomaa. Stationary vortex clusters in nonrotating Bose–Einstein condensates. *Phys. Rev. A*, 71:033626, Mar 2005.
[50] A. V. Murray, A. J. Groszek, P. Kuopanportti, and T. Simula. Hamiltonian dynamics of two same-sign point vortices. *Phys. Rev. A*, 93:033649, Mar 2016.
[51] R. Navarro, R. Carretero-González, P. Torres, P. Kevrekidis, D. Frantzeskakis, M. Ray, E. Altuntaş, and D. Hall. Dynamics of a few corotating vortices in Bose–Einstein condensates. *Phys. Rev. Lett.*, 110:225301, May 2013.
[52] T. Neely, E. Samson, A. Bradley, M. Davis, and B. Anderson. Observation of vortex dipoles in an oblate Bose–Einstein condensate. *Phys. Rev. Lett.*, 104:160401, Apr 2010.
[53] M. Pausch, F. Grossmann, B. Eckhardt, and V. G. Romanovski. Groebner basis methods for stationary solutions of a low-dimensional model for a shear flow. *Journal of nonlinear science*, 24(5):935–948, 2014.
[54] C. J. Pethick and H. Smith. *Bose–Einstein Condensation in Dilute Gases*. Cambridge University Press, Cambridge, UK, 2002.
[55] L. M. Pismen. *Vortices in Nonlinear Fields*. Oxford University Press, Clarendon, UK, 1999.
[56] L. Pitaevskii and S. Stringari. *Bose–Einstein Condensation*. Oxford University Press, Oxford, UK, 2003.

[57] A. Sadeghimanesh and E. Feliu. Groebner bases of reaction networks with intermediate species. *arXiv preprint arXiv:1804.01381*, 2018.
[58] E. Samson, K. Wilson, Z. Newman, and B. Anderson. Deterministic creation, pinning, and manipulation of quantized vortices in a Bose–Einstein condensate. *Phys. Rev. A*, 93:023603, Feb 2016.
[59] J. Seman, E. Henn, M. Haque, R. Shiozaki, E. Ramos, M. Caracanhas, P. Castilho, C. Castelo Branco, P. Tavares, F. Poveda-Cuevas, G. Roati, K. Magalhães, and V. Bagnato. Three-vortex configurations in trapped Bose–Einstein condensates. *Phys. Rev. A*, 82:033616, Sep 2010.
[60] Y.-i. Shin, M. Saba, M. Vengalattore, T. Pasquini, C. Sanner, A. Leanhardt, M. Prentiss, D. Pritchard, and W. Ketterle. Dynamical instability of a doubly quantized vortex in a Bose–Einstein condensate. *Phys. Rev. Lett.*, 93:160406, Oct 2004.
[61] A. Sommese and C. Wampler. *The Numerical solution of systems of polynomials arising in engineering and science*, volume 99. World Scientific, 2005.
[62] B. Sturmfels. *Algorithms in invariant theory*. Texts and Monographs in Symbolic Computation. SpringerWienNewYork, Vienna, second edition, 2008.
[63] G. Theocharis, D. Frantzeskakis, P. Kevrekidis, B. A. Malomed, and Y. S. Kivshar. Ring dark solitons and vortex necklaces in Bose–Einstein condensates. *Phys. Rev. Lett.*, 90:120403, Mar 2003.
[64] S. Xie, P. G. Kevrekidis, and T. Kolokolnikov. Multi-vortex crystal lattices in Bose–Einstein condensates with a rotating trap. *Proceedings of the Royal Society of London A: Mathematical, Physical and Engineering Sciences*, 474(2213), 2018.

Department of Mathematics, University of York, York, YO10 5DD, UK

Email address: emilie.dufresne@york.ac.uk

Mathematical Institute, University of Oxford, Andrew Wiles Building, Radcliffe Observatory Quarter, Woodstock Road, Oxford, OX2 6GG

Email address: harrington@maths.ox.ac.uk

Department of Applied and Computational Mathematics and Statistics, University of Notre Dame, Notre Dame, IN 46556, USA

Email address: hauenstein@nd.edu

Department of Mathematics and Statistics, University of Massachusetts Amherst, Amherst, MA 01003-4515, USA

Email address: kevrekid@math.umass.edu

School of Mathematical Sciences, University of Nottingham, University Park, Nottingham, NG7 2RD

Email address: paotripoli@gmail.com

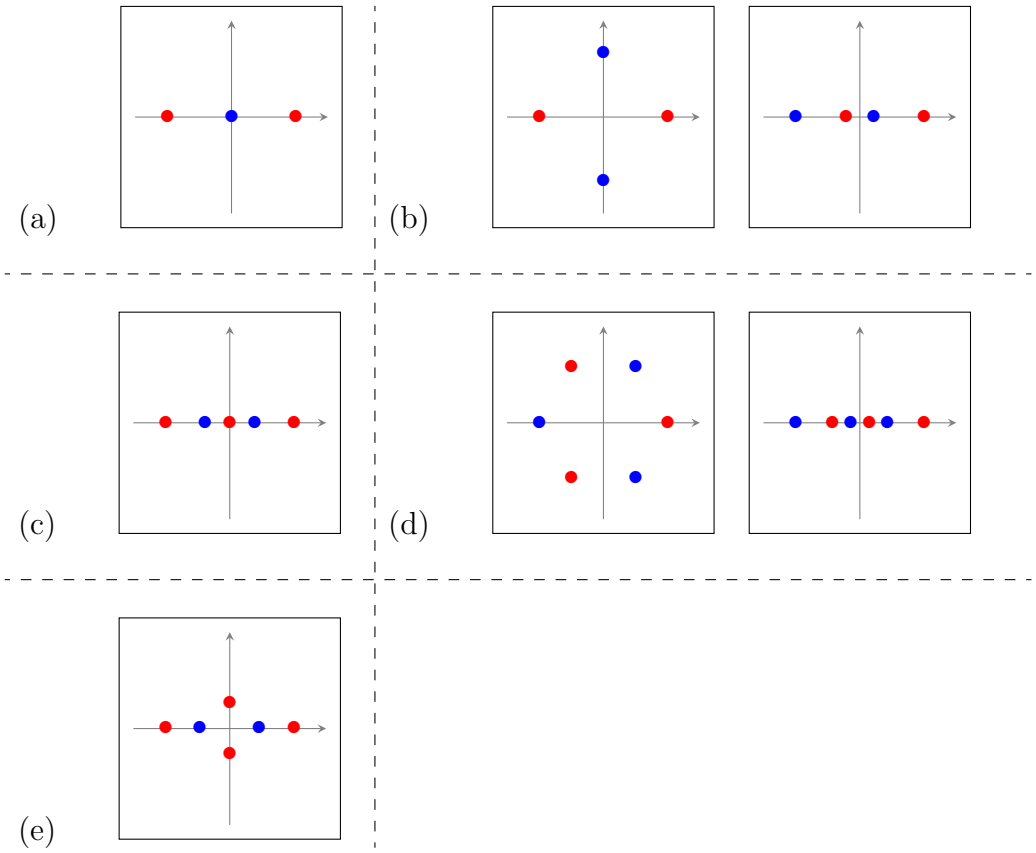

FIGURE 1. The solutions to the vortex problem for: $M = 2$, $N = 1$, (a); $M = 2$, $N = 2$, (b); $M = 3$, $N = 2$, (c); $M = 3$, $N = 3$, (d); $M = 4$, $N = 2$, (e).

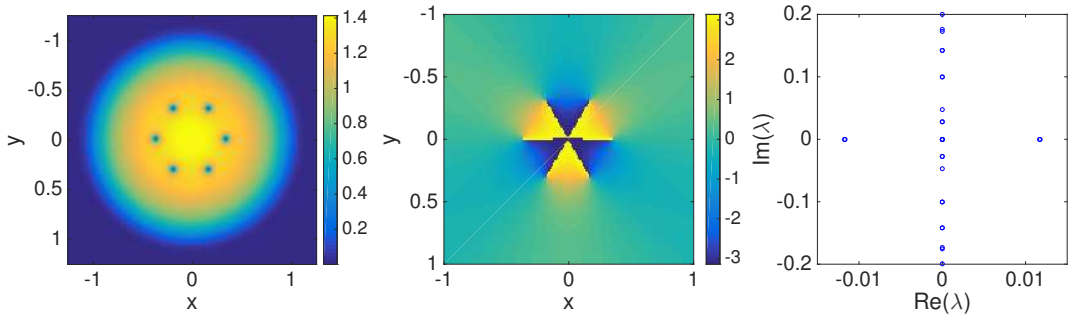

FIGURE 2. The first panel shows the density field $|u|^2$ from a PDE computation of Equation (1) involving $M = N = 3$ vortices in a hexagonal configuration. This is shown by a two-dimensional contour plot in the (x, y) plane. The second panel illustrates the corresponding phase, revealing the alternating nature of the charges. Finally, the third panel illustrates the results of the linear stability analysis around such a configuration. The spectral plane (λ_r, λ_i) of the associated linearization is illustrated for the corresponding eigenvalues $\lambda = \lambda_r + i\lambda_i$. The presence of two pairs of purely real eigenvalues establishes the exponential instability of such a solution.

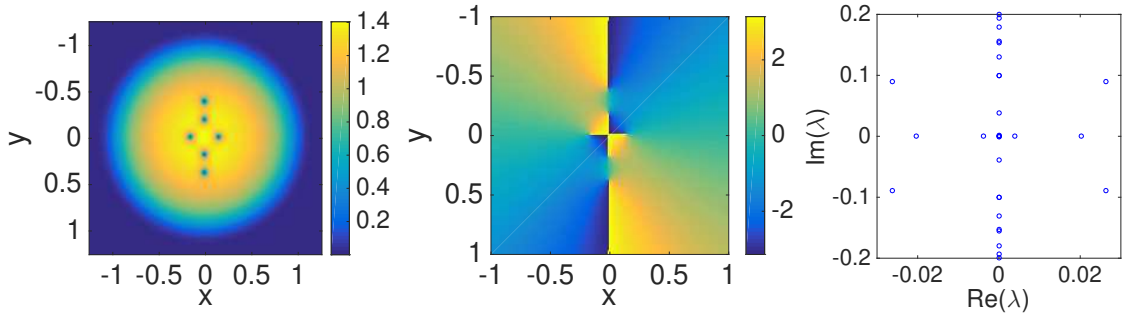

FIGURE 3. Same as the previous configuration, but now for the principal configuration discovered herein, namely the stationary solutions involving $M = 4$ positive and $N = 2$ negative charges. For details regarding the positions of the vortices and the comparison with the corresponding theoretical prediction, see the text. The last panel showcases the instability of this newly established configuration, by virtue of showing its two pairs of real eigenvalues (exponential instabilities) and one pair of complex eigenvalues (oscillatory instability).